

SOLID STATE ^{13}C MAS NMR INVESTIGATIONS OF AMORPHOUS CARBON THIN FILMS

Structural Changes During Annealing

Todd M. Alam, Tom A. Friedmann, and Amy J. G. Jurewicz*

1. INTRODUCTION

Thin films of hard amorphous carbon continue to gain importance in an increasing range of technologies and applications. Solid state ^{13}C magic angle spinning (MAS) nuclear magnetic resonance (NMR) spectroscopy has proven to be a powerful tool in the investigation of the local structure in amorphous carbon films. The majority of these ^{13}C MAS NMR investigations have focused on hydrogenated diamond-like carbon films.¹⁻¹³ Investigations of natural and synthetic diamonds,¹⁴⁻¹⁷ as well as graphite and graphite intercalation compounds have also been reported.^{18, 19} Recently, more unusual carbon forms have been probed using ^{13}C MAS NMR, including studies of pressure/temperature-treated C_{60} ,²⁰ two-dimensional polymerized C_{60} phases,²¹ and nanodiamonds produced during explosive compression.²²

One of the major benefits from these ^{13}C MAS NMR investigations is the ability to quantify the relative concentration of sp^3 (diamond-like) and sp^2 (graphite-like) carbons within the amorphous films. In hydrogenated carbon films it is found that the sp^2/sp^3 ratio is strongly dependent on the film preparation conditions, including: the self-bias voltage used in radio frequency discharge techniques,^{3, 5} plasma polymerization power levels,^{4, 8} gas flow rates, and starting constituent concentrations.^{1, 4, 8} For hydrogenated carbon films it has been shown that the optical band gap is controlled by the sp^2/sp^3 ratio,¹ while the film hardness and density correlates with the incorporated hydrogen content and average atomic constraint.^{1, 3, 5} The effects of thermal annealing on the local structure in amorphous hydrogenated carbon thin films have also been investigated using ^{13}C NMR.⁹

* Todd M. Alam, Department of Organic Materials, Sandia National Laboratories, Albuquerque, NM 87185-0888. Tom A. Friedmann, Department of Nanostructure and Semiconductor Physics, Sandia National Laboratories, Albuquerque, NM 87185-1415. Amy J. G. Jurewicz, Asteroids, Comets and Satellites Research Element, California Institute of Technology/Jet Propulsion Laboratory, Pasadena, CA 91109-8099.

Solid state ^{13}C MAS NMR investigation of amorphous carbon films which do not contain a significant hydrogen component are more limited. In particular, in non-hydrogenated carbon films there have been no NMR investigations into the effects of annealing or variations in preparation conditions on the local structure. In the work described here, solid state ^{13}C MAS NMR will be used to study the structural variations in an amorphous carbon thin film as a function of high temperature annealing. By utilizing a fully enriched ^{13}C source to grow the carbon films, two-dimensional (2D) NMR techniques can be performed that are not possible for natural abundance carbon films. Specific questions about the nature of the line broadening of the observed ^{13}C MAS NMR resonances will be addressed using a 2D MAS NMR exchange experiment.

2. EXPERIMENTAL

2.1. Thin Film Preparation

The amorphous carbon (a-C) thin films were prepared by pulsed laser deposition as previously described.²³ Briefly, an excimer laser (284nm KrF) was used to ablate a graphite target in a UHV-capable vacuum chamber. For the samples investigated here, a high laser fluence ($>100\text{ J/cm}^2$) was employed which resulted in the samples having a high concentration ($>50\%$) of 4-fold bonded carbons. ^{13}C enriched targets suitable for ablation are not commercially available, and the fully enriched (99%) ^{13}C carbon powder used (Cambridge Isotopes, Inc.) is impossible to press directly into a dense graphite target. Accordingly, the powder was first vacuum hot-pressed into pellets $\sim 40\%$ to 60% dense. The pellets were then machined to fit into experimental ultra-high pressure assemblies, outgassed under vacuum, cooled to room temperature and stored under argon, and then pressed to a density near graphite (2.2 g/cm^3) using a commercial tetrahedral-anvil apparatus (US Synthetic Corporation, UT). The resultant wafers were again stacked into ultra-high pressure assemblies, and the process repeated to produce a ^{13}C -enriched target of sufficient thickness. Therefore the ^{13}C powder was exposed to pressure-temperature conditions near the graphite-diamond phase boundary at least twice during the target synthesis. We believe this is the first time that a fully enriched ^{13}C a-C sample has been grown.

The a-C films were deposited on both sides of a thin ($100\mu\text{m}$) polished 2 inch Si(100) wafer to give a $3\mu\text{m}$ thickness (total $6\mu\text{m}$ summing both sides). To achieve this thickness, repeated deposition and annealing steps were used. First a $0.1\mu\text{m}$ ^{13}C enriched a-C layer was deposited followed by annealing at $650\text{ }^\circ\text{C}$ under argon to reduce the residual stress. This initial layer was followed by 6 additional layers of $0.5\mu\text{m}$, each with an annealing step at $650\text{ }^\circ\text{C}$ to reduce the residual stress. Annealing at $650\text{ }^\circ\text{C}$ has been shown not to have any major effects on the bonding and tribological properties of the films.²⁴ The Si wafer was then coarsely crushed for the MAS NMR analysis. During crushing it was observed that some of the carbon film delaminated from the substrate indicating that the residual stresses were not completely removed. Following the initial NMR studies a portion of the sample was further annealed under vacuum at temperatures ranging from $800\text{ }^\circ\text{C}$ to $900\text{ }^\circ\text{C}$ for varying times, and then reanalyzed by ^{13}C MAS NMR. It should be emphasized that these high temperature annealing steps were performed on samples that had already been annealed at $650\text{ }^\circ\text{C}$ during preparation.

2.2. Solid State NMR

The solid state ^{13}C MAS spectra were obtained at 100.1 MHz using a Bruker AMX400 NMR spectrometer. All spectra were obtained using a 4 mm broadband MAS probe, a $3.5\ \mu\text{s}$ $\pi/2$ pulse, with spinning speeds between 12.5 and 15 kHz. Direct polarization Bloch decay spectra were acquired using a 5s recycle delay, 8K scan averages. Spectra were obtained both with and without ^1H high power decoupling; no differences were observed in the resulting spectra. The CPMAS spectra were acquired with contact times ranging from $500\ \mu\text{s}$ to 2ms using 16K scan averages. For the results presented here approximately 100-150 mg of the crushed a-C/Si film were packed into zirconia rotors. In the situation where insufficient sample volume was available to completely fill the rotor, KBr or KI spacers were utilized, as these materials do not produce a background ^{13}C signal. We have shown that Teflon spacers can produce a significant ^{13}C background signal depending on the quality of the Teflon material utilized, so these spacers were not employed.

The two-dimensional (2D) ^{13}C NMR spectra were obtained under high speed MAS (12.5 kHz) using the pulse sequence shown in Figure 1.²⁵ The 2D data was acquired using a 5 s recycle delay, 1024 scan averages, with 4K complex points in the observed or t_2 dimension. The t_1 dwell was $9.3\ \mu\text{s}$ with 1024 time increments. The phase cycling utilized selects the ± 1 coherence in the t_1 dimension, with a time-proportional phase increment (TPPI) applied to produce an amplitude-modulated time-domain signal. This technique allows for pure absorptive and phase sensitive 2D spectra to be obtained.²⁶

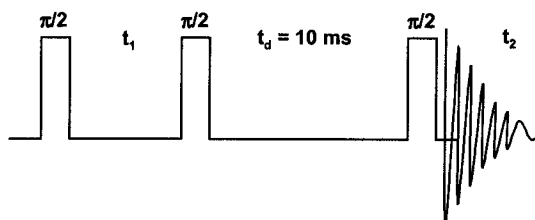


Figure 1. The 2D MAS NMR pulse sequence used to address the question of inhomogeneous broadening in the ^{13}C MAS spectra of the amorphous carbon films. By utilizing a short exchange time ($t_d = 10\ \text{ms}$), dipolar magnetization exchange between different ^{13}C nuclei is suppressed at sufficiently rapid spinning speeds, thereby providing a second dimension for increased spectral resolution.

3. RESULTS

3.1. Determination of local structure

The ^{13}C MAS NMR spectrum of the amorphous carbon film annealed at $650\ ^\circ\text{C}$ during film preparation is shown in Figure 2a. Two broad isotropic resonances are observed at $+68\ \text{ppm}$ and $+138\ \text{ppm}$, and are assigned to carbon species with 4-fold (sp^3) and 3-fold (sp^2) bonding environments. The signal to noise ratio realized in Figure 2 has

not been obtained for any previous investigations of amorphous carbon films. Similar chemical shifts have been reported previously for ^{13}C MAS NMR investigations of amorphous carbon films.^{11, 13} The ^{13}C NMR chemical shifts for crystalline diamond occur between +34 and +39 ppm,^{15, 16} while the chemical shift for crystalline graphite occur between +119 and +135 ppm.^{18, 19, 27} The dashed lines in Figure 2a designate these chemical shifts. The large difference between the observed sp^3 carbon chemical shift (Figure 2a) and the chemical shifts reported for crystalline diamond has been attributed to the amorphisation of the diamond species.¹³ Golzan and co-workers¹³ based this argument on the effect of amorphisation in silicon which produces an upfield shift of 37 ppm.²⁸ Recent *ab initio* molecular dynamic simulations of amorphous carbon predict a ^{13}C chemical shift of +75 ppm for 4-fold bonded carbons.²⁹ These simulations support the assignment of the +68 ppm resonance as amorphous sp^3 (diamond-like) carbons. The cross polarization (CP) MAS NMR spectra (not shown) shown no observable signal, even following extensive signal averaging. CPMAS utilizes the polarization of protons within the material to produce a ^{13}C NMR signal. The lack of any observable CP signal supports the conclusion that there is not any significant proton concentration within the film, in contrast to the CPMAS NMR results reported by Golzna *et al.* in similar carbon films.¹³ Hydrogen contents as low as 2 ppm have been measured in our films grown under UHV conditions. Given the conditions of the film preparation this inability to detect hydrogen constituents using CPMAS NMR is not surprising.

Simulation of the entire MAS manifold (Figure 2b) allows the relative fraction, the line width (FWHM = full width at half maximum) of the different carbon species, along with the sp^2/sp^3 ratio to be determined. These results are given in Table 1. Both the sp^2 and the sp^3 carbons show a significant anisotropy (or wide range) of the observed chemical shift, leading to a series of spinning side bands in the ^{13}C MAS NMR spectrum (Figure 2a). Previous investigations have also noted this anisotropy, and have proposed a variety of different explanations including, chemical shift anisotropy (CSA), inhomogeneous paramagnetic broadening, or ^{13}C - ^{13}C dipolar coupling.^{2, 7, 9, 17} For the spinning speeds employed (12.5 to 14 kHz) the CSA interaction is expected to be partially averaged, and is consistent with the spinning sideband pattern observed in Figure 2a. The graphite-like sp^2 carbons are expected to show the largest anisotropy, with a symmetric CSA on the order of ~ 178 ppm.³⁰ In investigations of amorphous carbon films Pan *et al.* observed spinning side bands over a range of about 50 kHz, which they concluded could only result from paramagnetic interactions.⁷ In studies of hydrogenated carbon films Lukins *et al.* made a similar argument.⁹ In the present investigation the existence of these very large interactions was not observed, supporting the conclusion that inhomogeneous paramagnetic interactions are not responsible for the observed side bands. In a later investigation of ^{13}C enriched diamond films, Pruski *et al.* attributed the spinning side band manifold to ^{13}C - ^{13}C homonuclear coupling on the order of 10 kHz.¹⁷ For the amorphous carbon films used in the present study we estimate that for fully ^{13}C enriched films the ^{13}C - ^{13}C homonuclear interaction would be on the order of 10 to 12 kHz, consistent with the observed sidebands in Figure 2a. The origin and characterization of this anisotropy in the chemical shift within amorphous carbon films will be detailed in a later publication. We note that the presence of these spinning side bands requires a complete MAS line shape analysis, as well as sufficient spinning speed to assure accurate determination of the relative carbon populations. For the magnetic field employed here (9.4 T) this required spinning speeds greater than ~ 12.5 kHz to assure that the ± 1

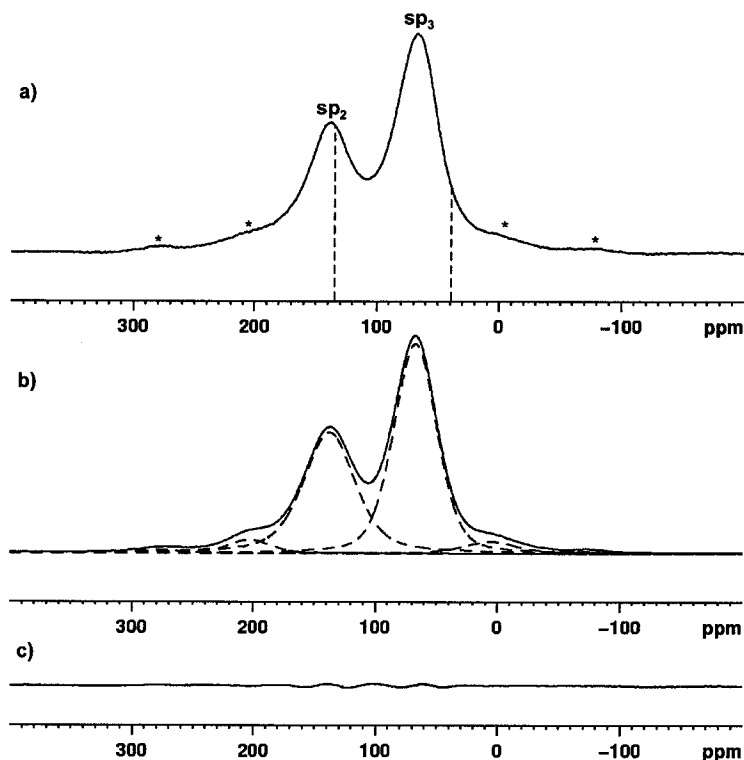


Figure 2. The a) experimental and b) simulated single pulse Bloch decay ^{13}C MAS NMR spectrum (spinning at 14 kHz) for an amorphous diamond thin film annealed at 650 °C. The residual between the experimental and the simulation is shown in c). Broad isotropic resonances for both the sp^3 and sp^2 type carbon species are observed. The dash vertical lines at $\delta = +135$ and $+39$ ppm show the chemical shifts of crystalline graphite and diamond, respectively, while the stars designate the spinning sidebands. The complete MAS simulations (—) shown in b) include both the isotropic resonance and the ± 1 spinning sideband manifold.

spinning side bands of either the sp^3 or the sp^2 resonance does not fall under the neighboring isotropic resonance. Failure to achieve fast enough spinning would mean that a portion of the sp^2 isotropic peak intensity would result from the +1 spinning side band of the sp^3 resonance. Similarly, a portion of the sp^3 resonance peak intensity would result from the -1 spinning side band of the sp^2 resonance. Errors as large as 10% can be introduced by not including the entire spinning side band manifold, or incidental overlap of the sidebands with the isotropic resonance. Future analysis of the relative fraction of sp^2 and sp^3 population should take these experimental difficulties into consideration.

To address the importance of variation in paramagnetic susceptibility, the temperature dependence of the ^{13}C MAS NMR chemical shifts were also determined. In carbon based materials this paramagnetic susceptibility should obey a Curie law and be

Table 1. The ^{13}C MAS NMR isotropic chemical shifts, line widths, and relative percent concentrations for amorphous carbon thin films as a function of annealing conditions

Sample ^a	δ (ppm) ^b	FWHM ^c (Hz)	f (%) ^d	sp ² /sp ³	N_{av} ^e
650 °C Annealed	67.5	4152	56.1	0.78	3.6
	137.8	5012	43.9		
+2 hrs. 800 °C	65.1	4045	46.9	1.13	3.5
	132.7	5638	53.1		
+2 hrs. 800/900 °C ^f	66.2	3431	21.1	3.74	3.2
	124.3	6118	78.9		
+4 hrs. 900 °C	63.8	3341	13.0	6.69	3.1
	123.0	6952	87.0		

^a Sample preparation conditions listing the annealing times and temperatures performed in addition to the original 650 °C annealing during film deposition.

^b The ^{13}C isotropic chemical shift referenced to the carbonyl resonance of the solid external secondary reference glycine ($\delta = +176.0$ ppm with respect to TMS $\delta = 0.0$ ppm).

^c Line width, full width at half maximum = FWHM.

^d Relative percent fraction obtained from full MAS spectral deconvolution. Estimated error $\pm 2\%$.

^e N_{av} = average bond number.

^f This sample was annealed 2 hours at 800 °C, followed by 2 hours at 900 °C.

strongly temperature dependent.³¹ The ^{13}C MAS NMR spectrum for the 650 °C annealed film obtained at 100 °C (not shown) is nearly identical to Figure 2a, showing a small 2 to 3 ppm shift relative to the ^{13}C chemical shift obtain at 25 °C (Table 1), demonstrating that there are no significant paramagnetic shifts in these carbon films.

The observation of the large line widths still needs to be addressed. In Figure 2a, the sp² carbon resonances has a FWHM = 4152 Hz (41.3 ppm), while the resonance of the sp³ carbon has a FWHM = 5012 Hz (49.8 ppm), respectively. Similar line widths have been observed in previous ^{13}C NMR investigation of amorphous carbon films.^{9, 10, 12, 13} The line widths for amorphous carbon films are consistently larger than that observed for crystalline diamond (~ 0.1 to 1 ppm). Several arguments have been proposed to explain these line widths including: (a) paramagnetic impurities and (b) chemical shift dispersion due to a range of structural variations within the carbon film.^{13, 16} While the relatively short spin-lattice relaxation times (T_{1Z}) in these films ($T_{1Z} = 21$ ms and 29 ms for sp³ and sp² carbons, respectively) can be attributed to relaxation with paramagnetic defect sites, Merwin *et al.* demonstrated that in synthetic diamonds this contribution to the line width is of minor importance in comparison to the chemical shift dispersion.¹⁶ To directly address if the observed line widths result from a distribution of carbon environments (or equivalently stress fluctuations) a 2D ^{13}C MAS NMR exchange experiment (Figure 1) was performed on the 650 °C annealed amorphous diamond thin film, and is shown in Figure 3. For the short mixing time (10 ms) and the high spinning speeds (12.5 kHz) employed, exchange due to ^{13}C - ^{13}C interactions are minimal. The chemical shift separation into the second dimension now allows individual slices (or 1D spectrum) through a given frequency to be obtained such that the residual homogenous broadening can be addressed. The resulting spectrum obtained by taking a slice through the maximum intensity of the sp³ resonance (+68 ppm) is shown in Figure 3 (middle), while the slice through the sp² (+138 ppm) resonance is shown on the bottom of Figure 3. Both

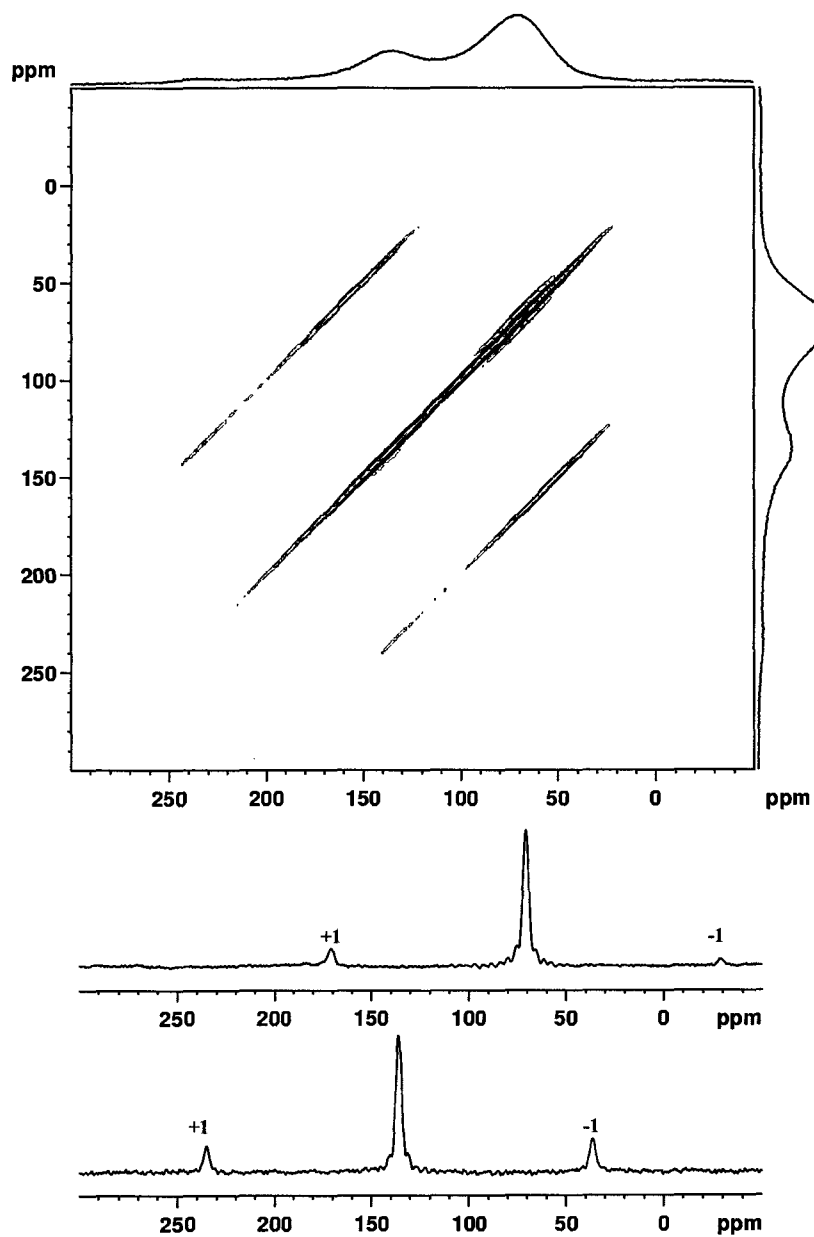


Figure 3. Contour plot (top) of the 2D ^{13}C MAS NMR spectrum for the 650 °C annealed amorphous carbon film. Slices through the isotropic sp^3 , +68 ppm (middle) and sp^2 , +138 ppm (bottom) resonances produce 1D spectrum for these individual frequencies, and reveal very narrow (~300 Hz) line widths, along with both the +1 and -1 spinning sidebands.

of these spectrum reveal a FWHM ~ 300 Hz (~ 3 ppm), which is over 10 times smaller than the FWHM observed in Figure 2a (see also Table 1). The resolution in the t_1 dimension is ~ 100 Hz, suggesting that the observed 300 Hz line width may result from residual ^{13}C - ^{13}C homonuclear dipolar coupling or exchange not suppressed by MAS.

This 2D MAS NMR experiment provides the first clear experimental evidence that both the sp^3 and sp^2 resonances are inhomogeneously broadened, with the broad lines resulting from the overlap of many individual sharp resonances with slightly different chemical shifts. This range of chemical shifts demonstrates that the NMR is detecting carbons within the film that have significantly different local structural environments. If the films were (a) highly ordered, (b) showed a uniform bonding motif, and (c) did not contain defects or edge effects then all the carbon atoms would show the same chemical shift. This is clearly not the case. Defects, vacancies, different bonding arrangements between the sp^2 and sp^3 carbons, variations in bond angles and bond lengths cause distortions within the film, and thereby lead to a range of observed chemical shifts. Presently there are few studies correlating variation in bond lengths and angle, or changes in the bonding arrangements with the observed ^{13}C NMR chemical shift in pure carbon films. Recently Mauri *et al.*²⁹ used density functional theory to predict the variation in ^{13}C chemical shift of diamonds as a function of volume (V) changes or applied pressure (P). The chemical shift varied linearly with volume as $d\delta/dV = 1.72$ ppm/(a.u.)³ and with pressure as $d\delta/dP = 0.30$ ppm/GPa. Using this relationship the observed line widths in these carbon films would correlate to a pressure distribution or pressure fluctuations on the order of ~ 138 GPa. It has yet to be determined if these *ab initio* results for the pressure-chemical shift correlation derived for crystalline diamond can be applied to mixed amorphous carbon films.

The concept of pressure-induced chemical shifts can be explored using the idea of *local atomic level stresses*.³² Using this model, local stresses at the atomic scale are caused by structural incompatibilities, and are therefore present both in any disordered system, and in materials where there exist non-equivalent atoms. Kelires and co-workers³³⁻³⁶ have performed extensive simulations of amorphous carbon films, and have argued that there are indeed local stresses resulting from disorder in the bond lengths and angles, as well as stresses resulting from the incompatibility between sp^2 and sp^3 carbon environments. It is possible that the average of the overall internal stress is zero even though there exist a wide range of local stresses. Kelires performed a series of Monte Carlo (MC) simulations using an empirical potential approach to describe the local stress in amorphous carbon films.³³⁻³⁵ They calculated a very large distribution of local internal stresses; the extremes of these distributions originating from carbon atoms with severely strained bond lengths and angles. In these simulations the sp^3 carbon atoms were found to be under compressive stress, while sp^2 atoms were under tensile stress. As a result the combination of bond types can relieve a portion of the internal strain energy found within the films.³³ For amorphous carbon films with a average bond number, $N_{av} = 3.5$, (similar to the 650 °C film, see Table 1) the MC simulations predicted a distribution of internal stresses on the order of ~ 60 Gpa.³³⁻³⁵ This predicted stress is approximately half as large as the stress obtained from the simple line width argument above (~ 138 Gpa), but it is still the same order of magnitude.

3.2. Structural variation with annealing

The ¹³C MAS NMR spectra for the a-C films as a function of annealing histories are shown in Figure 4. The NMR spectrum for the original a-C film that was annealed at 650 °C during preparation is shown in Figure 4a, with the spectrum for an a-C film following 2 hours of annealing at 800 °C in Figure 4b. The spectrum for an a-C film annealed for 2 hours at 800 °C, followed by an additional 2 hours of annealing at 900 °C is shown in Figure 4c. Finally the ¹³C MAS NMR spectrum for the a-C film following 4 hours of annealing at 900 °C is shown in Figure 4d. The resulting relative concentrations, line widths and sp²/sp³ ratios are given in Table 1.

Annealing at these high temperatures has a dramatic effect on the structural properties in these a-C films. The most prominent is the increased fraction of sp² (graphite-like) carbon species within the film. The sp²/sp³ ratio increases from 0.78 for the original 650 °C annealing to 6.69 following 4 hours of annealing at 900 °C (Table 1). This is consistent with an increase in the sp² fraction with annealing previously reported for hydrogenated carbon films, but the film in the previous investigation was essentially 100% sp² following annealing at only 500 °C.⁹ That previous work attributed the loss of the sp³ carbons to out gassing of hydrocarbons or to evolution of CO and CO₂ formed by reactions of the film with oxygen. In contrast, their mechanisms are unlikely to be operative for our materials because: (a) the carbon films used in the present investigation do not have significant hydrogen content, and (b) annealing was performed under vacuum, such that any oxygen involved in the conversion of sp³ to sp² carbon must arise from the original film, which would be minor. Aromatization is the dominant conversion mechanism in our experiment. This difference in the annealing mechanism accounts for the much higher temperatures required for significant conversion to sp² type carbons in comparison to hydrogenated amorphous carbon films. It is interesting to note that the film annealed for 2 hours at 800 °C, followed by annealing for 2 hours at 900 °C (Figure 4c) is distinct from the film annealed at 4 hours at 900 °C (Figure 4d). The kinetics for annealing at 900 °C is slow enough that 2 hours of annealing at this higher temperature is not sufficient to achieve an equilibrium state.

The average atomic coordination (N_{av}) also decreases steadily with annealing of the a-C film, changing from 3.6 for the 650 °C film to 3.1 for the 900 °C film. The N_{av} can be determined from the NMR data using the relationship:⁵

$$N_{av} = 4f(sp^3) + 3f(sp^2) \quad (1)$$

where $f(sp^3)$ and $f(sp^2)$ are the relative fraction of the 4-fold and 3-fold bonded carbon types within the film. Tamor *et al.* argued that in an optimally constrained network that N_{av} is exactly 2.4. Networks with larger N_{av} must therefore contain regions of local strain. For the films investigated, annealing reduces this overall constraint on the network (Table 1). It was pointed out by Tamor *et al.* that in over-constrained materials, it is possible for the material to possess no residual stress, as a result of over-constrained clusters being connected by less rigid connective tissue. This type of connectivity signifies a breakdown of the random network assumption.⁵ For the 900 °C annealed film the N_{av} value of 3.1 is significantly lower than the 3.45 value predicted from MC simulation of the annealing process in amorphous carbon films.³⁷

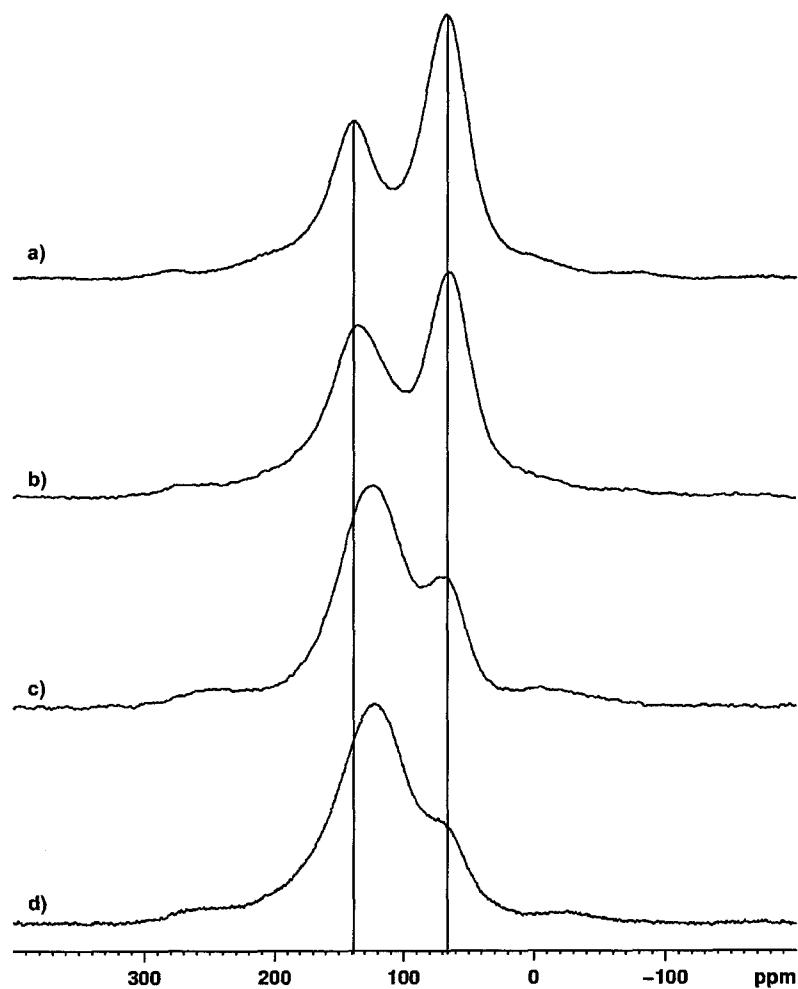


Figure 4. The ^{13}C MAS NMR spectra for an amorphous carbon film as a function of annealing conditions: a) 650 °C (during preparation), b) an additional 2 hours of annealing at 800 °C, c) 2 hours of annealing at 800 °C followed by 2 hours of annealing at 900 °C, and d) 4 hours of annealing at 900 °C. The vertical lines are for visual aid in clearly delineating the variation of the chemical shift as a function of annealing.

The ^{13}C NMR chemical shift of the sp^3 carbon species is essentially invariant to the annealing process, while the sp^2 carbon resonance shows a significant upfield shift of nearly +13 ppm to approximately +123 ppm (See Figure 4). Within the local stress model of Kelires described previously, this would imply that the average of all the local stresses for the sp^3 carbons remains unchanged with annealing. This observation also

suggest that the sp^2 bonding environment is more impacted by the change in the sp^2/sp^3 ratio, and may reflect a trend to form extended graphite-like structures at the higher ratios. The isotropic ^{13}C NMR chemical shift of crystalline graphite has been reported at $\delta = +119$ ppm.³⁰ The line width of the sp^3 carbon species decreases from 4152 Hz to 3341 Hz following annealing at 900 °C for 4 hours. In contrast, the line width of the sp^2 resonance increases from 5012 Hz to 6952 Hz during annealing. If the relationship between pressure and the variation in the diamond chemical shift (see section 3.1) is employed, then the decrease in the line width for the diamond-like sp^3 resonance would correspond to a reduction in the distribution of local atomic stresses by ~ 27 GPa. A similar correlation of chemical shift with pressure has not been determined for graphite. Therefore arguments correlating the effect of annealing on the line width of the sp^2 resonance with changes in the local atomic stresses are not presently possible.

4. CONCLUSIONS

The local structure in amorphous carbon was investigated using solid state ^{13}C MAS NMR, including the relative fraction of sp^2 and sp^3 carbon species. The use of 2D MAS exchange NMR provided experimental proof that the observed resonances are inhomogeneously broadened, and that the large observed line widths are a result of a dispersion of chemical shifts reflecting variations in the local structure (or equivalently variations in the internal pressure or volume). This distribution of chemical shifts can be understood using the concept of local atomic level internal stresses. For the original carbon film annealed at 650 °C, the large line width would predict a distribution of local stresses for the diamond-like carbons. The ^{13}C MAS NMR allowed us to observe a number of distinct structural changes within the amorphous carbon films caused by the annealing process. Heat treatment of our a-C films does increase the relative fraction of the sp^2 species, but requires a much higher temperature than that observed for hydrogenated carbon films. Accordingly, the sp^3 to sp^2 conversion mechanism in these carbon films is different from that previously observed in the hydrogenated films: here aromatization is the dominant conversion mechanism. The changes in the amorphous carbon film with annealing can also be related to local atomic level stresses. The distribution of local stresses in the sp^3 carbon environment is found to decrease by ~ 27 Gpa with annealing at 900 °C. An additional MAS NMR investigation into the extended medium-range order within these amorphous films is presently being pursued.

5. ACKNOWLEDGEMENTS

Sandia is a multiprogram laboratory operated by the Sandia Corporation, a Lockheed Martin Company, for the United States Department of Energy under Contract DE-AC04-94AL85000. A portion of this work (A.J.) was carried out through the Jet Propulsion Laboratory, California Institute of Technology, under contract with the National Aeronautics and Space Administration. Thanks to the Genesis Discovery Mission (especially Don Burnett, PI) who requested the development of the enriched ^{13}C target material.

Reference herein to any specific commercial product, process, or service by trade name, trademark, manufacturer, or otherwise, does not constitute or imply endorsement by the United States Government, or the Jet Propulsion Laboratory, California Institute of Technology.

6. REFERENCES

- (1) S. Kaplan, F. Jansen and M. Machonkin, Characterization of amorphous-hydrogen films by solid-state nuclear magnetic resonance, *Appl. Phys. Lett.* **47**(7), 750-753 (1985).
- (2) A. Grill, B. S. Meyerson, V. V. Patel, J. A. Reimer and M. A. Petrich, Inhomogeneous carbon bonding in hydrogenated amorphous carbon films, *J. Appl. Phys.* **61**(8), 2874-2877 (1987).
- (3) K. Yamamoto, Y. Ichikawa, T. Nakayama and Y. Tawada, Relationship between plasma parameters and carbon atom coordination in a-C:H films prepared by RF glow discharge decomposition, *Japanese J. Appl. Phys.* **27**(8), 1415-1421 (1988).
- (4) R. J. Gambogi, D. L. Cho, H. Yasuda and F. D. Blum, Characterization of plasma polymerized hydrocarbons using CP-MAS ^{13}C -NMR, *J. Poly. Sci., Part A: Poly. Chem.* **29**, 1801-1805 (1991).
- (5) M. A. Tamor, W. C. Vassell and K. R. Carduner, Atomic constraint in hydrogenated "diamond-like" carbon, *Appl. Phys. Lett.* **58**(6), 592-594 (1991).
- (6) R. Kleber, K. Jung, H. Ehrhardt, I. Mühlhling, K. Breuer, H. Metz and F. Engelke, Characterization of the sp^2 bonds network in a-C:H layers with nuclear magnetic resonance, electron energy loss spectroscopy and electron spin resonance, *Thin Solid Films* **205**, 274-278 (1991).
- (7) H. Pan, M. Pruski, B. C. Gerstein, F. Li and J. S. Lannin, Local coordination of carbon atoms in amorphous carbon, *Phys. Rev. B* **44**(13), 6741-6745 (1991).
- (8) G. Beamson, W. J. Brennan, N. J. Clayden and R. C. K. Jennings, Characterization of amorphous carbon films by ^{13}C CP MAS NMR Spectroscopy, *J. Poly. Sci., Part B: Poly. Phys.* **31**, 1205-1211 (1993).
- (9) P. B. Lukins, D. R. McKenzie, A. M. Vassallo and J. V. Hanna, ^{13}C NMR and FTIR study of thermal annealing of amorphous hydrogenated carbon, *Carbon* **31**(4), 569-575 (1993).
- (10) U. Schwerk, F. Engelke, R. Kleber and D. Michel, Characterization of hydrogenated amorphous carbon films by nuclear magnetic resonance techniques, *Thin Solid Films* **230**, 102-107 (1993).
- (11) C. Jäger, J. Gottwald, H. W. Spiess and R. J. Newport, Structural properties of amorphous hydrogenated carbon. III. NMR investigations, *Phys. Rev. B* **50**(2), 846-852 (1994).
- (12) R. H. Jarman, G. J. Ray, R. W. Standley and G. W. Zajac, Determination of bonding in amorphous carbon films: A quantitative comparison of core-electron energy-loss spectroscopy and ^{13}C nuclear magnetic resonance spectroscopy, *Appl. Phys. Lett.* **49**(17), 1065-1067 (1986).
- (13) M. M. Golzan, P. B. Lukins, D. R. McKenzie, A. M. Vassallo and J. V. Hanna, NMR evidence for strained carbon bonding in tetrahedral amorphous carbon, *Chem. Phys.* **193**, 167-172 (1995).
- (14) M. J. Duijvestijn, C. Van Der Lugt, J. Smidt and R. A. Wind, ^{13}C NMR spectroscopy in diamonds using dynamic nuclear polarization, *Chem. Phys. Lett.* **102**(1), 25-28 (1983).
- (15) P. M. Henrichs, M. L. Coffield, R. H. Young and J. M. Hewitt, Nuclear spin-relaxation via paramagnetic centers in solids. ^{13}C NMR of diamonds, *J. Magn. Reson.* **58**, 85-94 (1984).
- (16) L. H. Merwin, C. E. Johnson and W. A. Weimer, ^{13}C NMR investigation of CVD diamond: Correlation of NMR and Raman spectral linewidths, *J. Mater. Res.* **9**(3), 631-635 (1994).
- (17) M. Pruski, D. P. Lang, S.-J. Hwang, H. Jia and J. Shinar, Structure of thin diamond films: A ^1H and ^{13}C nuclear-magnetic-resonance study, *Phys. Rev. B* **49**(15), 10635-10642 (1994).
- (18) T. Tsang and H. A. Resing, ^{13}C nuclear magnetic resonance in graphite intercalation compounds, *Solid State Comm.* **53**(1), 39-43 (1985).
- (19) Y. Hiroshima and K. Kume, High resolution ^{13}C NMR spectra in graphite chemical shift and diamagnetism, *Solid State Comm.* **65**(7), 617-619 (1988).
- (20) Y. Maniwa, M. Sato, K. Kume, M. E. Kozlov and M. Tokumoto, Comparative NMR study of new carbon forms, *Carbon* **34**(10), 1287-1291 (1996).
- (21) A. Rezzouk, Y. Errammach, F. Rachdi, V. Agafonov and V. A. Davydov, High-resolution ^{13}C NMR studies of the tetragonal two-dimensional polymerized C_{60} phase, *Physic E* **8**, 1-4 (2000).
- (22) J.-B. Donnet, E. Fousson, L. Delmotte, M. Samirant, C. Baras, T. K. Wang and A. Eckhardt, ^{13}C NMR characterization of nanodiamonds, *C. R. Acad. Sci. Paris, Série IIc, Chimie* **3**, 831-838 (2000).
- (23) T. A. Freidmann, M. P. Siegal, D. R. Tallant, R. L. Simpson and F. Dominguez, in: *Novel Forms of Carbon II*, edited by C. L. Renschler, D. Cox, J. Pouch and Y. Achiba (Materials Research Society, Pittsburg, 1994), pp 501-506.

- (24) T. A. Friedmann, J. P. Sullivan, J. A. Knapp, D. R. Tallant, D. M. Follstaedt, D. L. Medlin and P. B. Mirkarimi, Thick stress-free amorphous-tetrahedral carbon films with hardness near that of diamond, *Appl. Phys. Lett.* **71**(26), 3820-3822 (1997).
- (25) T. M. Alam and R. K. Brow, Local structure and connectivity in lithium phosphate glasses: a solid-state ³¹P MAS NMR and 2D exchange investigation, *J. Non-Cryst. Solids* **223**, 1-20 (1998).
- (26) K. Schmidt-Rohr and H. W. Spiess, *Multidimensional solid-state NMR and polymers* (Academic Press, San Diego, 1994).
- (27) H. L. Retcofsky and R. A. Friedel, Carbon-13 magnetic resonance in diamonds, coals and graphite, *J. Phys. Chem.* **77**(1), 68-71 (1973).
- (28) W.-L. Shao, J. Shinar, B. C. Gerstein, F. Li and J. S. Lannin, Magic-angle spinning ²⁹Si NMR study of short-range order in α -Si, *Phys. Rev. B* **41**(13), 9491-9494 (1990).
- (29) F. Mauri, B. G. Pfrommer and S. G. Louie, *Ab initio* NMR chemical shift of diamond, chemical-vapor-deposited diamond, and amorphous carbon, *Phys. Rev. Lett.* **79**(12), 2340-2343 (1997).
- (30) H. A. Resing and D. L. VanderHart, Coronene as a model of charcoal: Calibration of the carbon-13 NMR shift tensor to count carbon atoms at the plane edge, *Zeitschrift für Physikalische Chemie Neue Folge* **151**, 137-155 (1987).
- (31) A. Abragam, *The principles of nuclear magnetism* (Clarendon Press, Oxford, 1961).
- (32) V. Vitek and T. Egami, Atomic level stresses in solids and liquids, *Phys. Stat. Sol. (B)* **144**, 145-156 (1987).
- (33) P. C. Kelires, Elastic properties of amorphous carbon networks, *Phys. Rev. Lett.* **73**(18), 2460-2463 (1994).
- (34) P. C. Kelires, Stress properties of diamond-like amorphous carbon, *Physica B* **296**, 156-162 (2001).
- (35) P. C. Kelires, Intrinsic stress and stiffness variations in amorphous carbon, *Diamond and Related Materials* **10**, 139-144 (2001).
- (36) M. Fyta and P. C. Kelires, Stress variations near surfaces in diamond-like amorphous carbon, *J. Non-Cryst. Solids* **266-269**, 760-764 (2000).
- (37) P. C. Kelires, Structural properties and energetics of amorphous forms of carbon, *Phys. Rev. B* **47**(4), 1829-1839 (1993).